Dynamics of Mutually Coupled VCSEL's

Raúl Vicente[a] and Claudio R. Mirasso[a,b]

[a]Departament de Física, Universitat de les Illes Balears, Crta. Valldemossa Km 7.5, E-07122, Palma de Mallorca, Spain;
[b]Electrical Engineering Department, University of California, Los Angeles, Los Angeles, CA, 90095-1594, USA

ABSTRACT

We study the dynamics of two Vertical Cavity Surface Emitting Lasers (VCSEL's), when they are bidirectionally coupled through the mutual injection of their coherent optical fields. In the long distance limit between the lasers, we focus on the Low Frequency Fluctuations (LFF) regime and we investigate the polarization-resolved dynamics of each laser under the effect of detuning. In the short distance limit, the influence of the propagation phase parameter is also evaluated. For large spin-flip rates, it is found that a change in the propagation phase may induce a sudden switch in the polarization mode that becomes dominant. Extensive simulations scanning the Coupling-Detuning space are performed for both long and short injection delay times.

Keywords: Semiconductor Lasers, VCSEL, Delay, Bidirectional Coupling.

1. INTRODUCTION AND MODEL

The nonlinear dynamics of VCSEL's subject to external perturbations has been studied for a long time. Conventional optical feedback, polarization selected or rotated optical feedback and unidirectional optical injection[1–3] are among the most popular schemes for investigating the dynamical response of the VCSEL. High frequency polarization modulation and polarization switching has been achieved with the use of the former setups. Much less common in the literature are the works concerning to the mutual injection of two VCSEL's in a face to face configuration, where the experimental results obtained by Ohtsubo and collaborators[4] demonstrated that chaotic synchronization between one mode (the $\hat{x}$-mode) of each laser could be attained. However, an exhaustive investigation of the synchronization properties of this system still lacks to be done. This work is indeed devoted to characterize the influence of several operating and internal parameters on the dynamics and synchronization of two mutually coupled VCSEL's.

The modeling of the setup is performed at the level of modified rate equations, under the framework of the Spin-Flip-Model (SFM)[5] for the individual dynamics of each VCSEL. After the adiabatic elimination of the material polarization and considering moderate values of the coupling constant (in order to avoid higher order reflection terms), the equations governing the fields and carrier numbers inside each laser are

$$\dot{E}_{1\pm} = -i\Delta E_{1\pm} + \kappa(1+i\alpha)\left[N_1 \pm n_1 - 1\right]E_{1\pm} - (\gamma_a + i\gamma_p)E_{1\mp} + \xi e^{-i\Omega\tau}E_{2\pm}(t-\tau) + F_{1\pm}(t), \quad (1)$$

$$\dot{N}_1 = -\gamma_e\left[N_1 - \mu + (N_1+n_1)|E_{1+}|^2 + (N_1-n_1)|E_{1-}|^2\right], \quad (2)$$

$$\dot{n}_1 = -\gamma_s n_1 - \gamma_e\left[(N_1+n_1)|E_{1+}|^2 + (N_1-n_1)|E_{1-}|^2\right], \quad (3)$$

$$\dot{E}_{2\pm} = i\Delta E_{2\pm} + \kappa(1+i\alpha)\left[N_2 \pm n_2 - 1\right]E_{2\pm} - (\gamma_a + i\gamma_p)E_{2\mp} + \xi e^{-i\Omega\tau}E_{1\pm}(t-\tau) + F_{2\pm}(t), \quad (4)$$

$$\dot{N}_2 = -\gamma_e\left[N_2 - \mu + (N_2+n_2)|E_{2+}|^2 + (N_2-n_2)|E_{2-}|^2\right], \quad (5)$$

$$\dot{n}_2 = -\gamma_s n_2 - \gamma_e\left[(N_2+n_2)|E_{2+}|^2 + (N_2-n_2)|E_{2-}|^2\right]. \quad (6)$$

Further author information: (Send correspondence to R.V.)
R.V.: E-mail: raulv@imedea.uib.es, Telephone: 34 971172505

where the electrical fields $E_\pm$ are written in the circular basis and both lasers are taken identical, except for a possible mismatch between their free-running optical frequencies ($\Delta = \frac{\omega_2-\omega_1}{2}$, $\Omega = \frac{\omega_2+\omega_1}{2}$). In order to simplify the model, the transverse mode structure has not been considered here. Another important assumption made in the equations, is the perfect alignment between both lasers with respect to their two preferred orthogonal orientations for the optical field, $\hat{x}$ and $\hat{y}$. In the former equations, N represents the total inversion population while n is the difference in population inversions of the two spin channels associated to the emission of opposite circularly polarized photons in the SFM description. The last term in the field equations accounts for the Langevin noise sources associated to the spontaneous emission processes $F_\pm(t) = \sqrt{\beta\gamma_e(N \pm n)}\chi_\pm$, where for each noise realization $\chi_\pm$ are two independent complex random numbers with zero mean and δ-correlated. Typical values of the parameters appearing in (1-6) that will be used throughout this paper are collected in Table 1.

Parameter	Meaning	Value
α	Henry's linewidth enhancement factor	3
κ	field decay rate	300 ns^{-1}
γ_e	total carrier number decay rate	1 ns^{-1}
γ_s	spin-flip rate	50-400 ns^{-1}
γ_a	amplitude anisotropy	-0.1 ns^{-1}
γ_p	phase anisotropy	3 ns^{-1}
μ	normalized pump	1-1.5
ξ	coupling strength	0-30 ns^{-1}
τ	injection delay time	0.2-4 ns
$\Delta\nu$	frequency detuning	0-10 GHz
β	spontaneous emission factor	0-1$\times 10^{-5}$

Table 1. Range of values used in this work for the parameters appearing in equations (1-6).

The rest of the paper is organized as follows. Section 2 deals with the modification of the LFF behavior displayed by both polarizations in the appropriate conditions, when a detuning is present in the system. Section 3 shows the effect of changing the propagation phase between the VCSEL's in the polarization resolved dynamics and how the spin-flip rate modifies these results. In Section 4 we discuss the possible dynamical states of the coupled system as function of the detuning and coupling coefficients. Finally, a brief summary and future perspectives are elucidated in the Conclusions section.

2. LOW FREQUENCY FLUCTUATIONS STATES

When two long-separated mutually coupled Edge Emitting Semiconductor Lasers (EESL) are both pumped close to their solitary threshold, they use to enter in the so-called Low Frequency Fluctuations regime. It is also known that the effect of the detuning on the system is to induce a leader-laggard synchronization between the two optical fields.[6] However, in the present situation, it naturally arise the question of the role of each polarization in the synchronization process, which has not counterpart in the EESL case. So, in order to illustrate the polarization resolved contribution to the LFF dynamics, we plot in Figure 1 typical traces of the $\hat{x}$ and $\hat{y}$ polarized intensities for several values of the detuning parameter. All temporal series have been smoothened with a fifth-order Butterworth filter with a high cut-off frequency of 100 MHz.

In the case of low spin-flip rate, at zero detuning (a), only the high frequency mode of each laser ($\hat{x}$-mode) starts lasing, exhibiting the typical achronal synchronized LFF traces. As usual, the cross-correlation function $\sigma(\Delta t)$ shows two maximum peaks at $\pm\tau$ with a correlation coefficient of $\sigma(\pm\tau) \approx 0.87$. Increasing the detuning (b), we find that the low frequency mode starts to get active taking the principal role in the low frequency dynamics. Now, the $\hat{x}$-modes of both lasers show a worse lag synchronization quality than in the previous case $\sigma(\pm\tau) \approx 0.63$, while the $\hat{y}$-modes cross-correlation at $\pm\tau$ takes a value of 0.92. In the dropouts sequence, it is observed that is the dominant mode of the laser with higher frequency who drops first. Further increasing

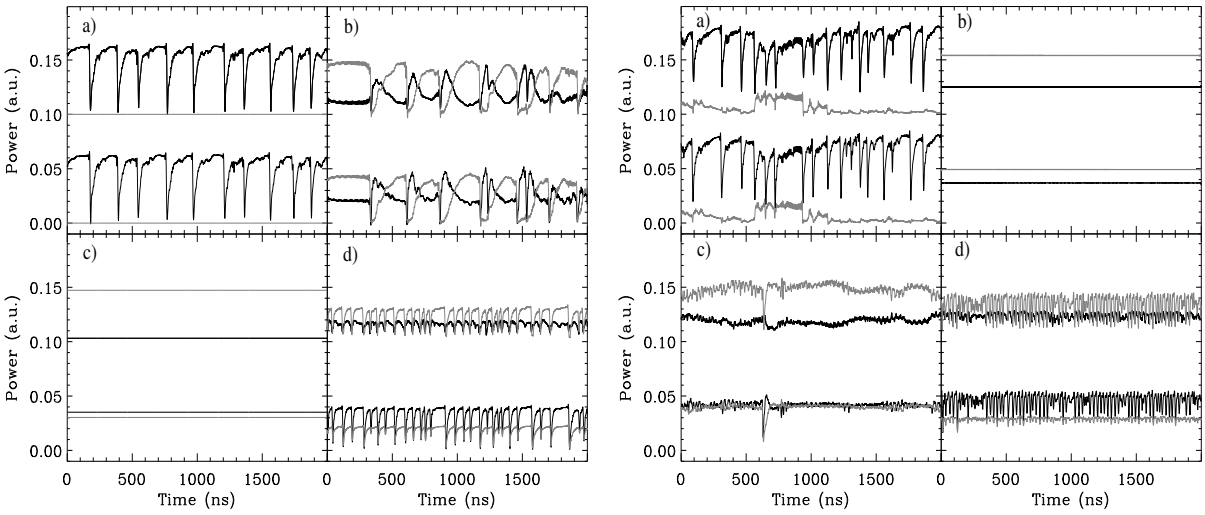

Figure 1. Detuning effect on the LFF. Time traces for the $\hat{x}$ ($\hat{y}$) polarized intensities are plotted in black (grey) Series corresponding to the laser 1 has been vertically shifted for clearness reasons. The left panel contains simulations performed with $\gamma_s = 50$ ns^{-1} and $\mu = 1.01$, while in the right panel $\gamma_s = 400$ ns^{-1} and $\mu = 1.03$, have been used. a) $\Delta\nu = 0$ GHz, b) $\Delta\nu = 3$ GHz, c) $\Delta\nu = 6$ GHz and d) $\Delta\nu = 10$ GHz. Other parameters are $\xi = 15$ ns^{-1} and $\tau = 4$ ns.

the frequency mismatch (c), the system enters into a stable locking area where a constant output power is achieved for the different polarizations. In particular, it is noticed that for the laser 2 (higher frequency laser), the dominant mode is the $\hat{x}$-mode, whereas for the laser 1 (lower frequency laser) is the $\hat{y}$-mode the one that is extracting more optical power. For detunings as large as 10 GHz (d), it turns out that the dominant modes of each laser are nearly perfectly correlated with lag τ, what implies a synchronization between the $\hat{y}$-mode of the laser 1 with the orthogonally oriented $\hat{x}$-mode of the laser 2. Regarding the synchronization of $\hat{x}$ and $\hat{y}$-modes belonging to the same VCSEL, it is worth to mention the excellent zero-lagged synchronization achieved by these two modes in the higher frequency laser ($\sigma(0) = 0.96$). A worse correlation value is obtained for $\hat{x}$ and $\hat{y}$-modes associated to the lower frequency laser. It is also worth to mention the reduction of time between consecutive dropout events for large detuning values.

For the large spin-flip rate case, it was necessary to increase the pump value considered previously, in order to enter in the LFF regime. Nevertheless, the main features of the before-mentioned characteristics are also shared in this case. Now, the principal differences observed are that the locking state is reached for smaller values of the detuning and that some irregular oscillations appear for intermediate detunings.

Finally, we show in Figure 2 the optical spectra corresponding to the locking state observed in the left panel of Figure 1. Here, the mutual frequency pulling and pushing effects shift all the present polarization modes ($\hat{x_1}, \hat{y_1}, \hat{x_2}$ and $\hat{y_2}$) to lock to a relative optical frequency around -6 GHz, nearly coinciding with the original frequency mismatch $\Delta\nu$.

3. PHASE PROPAGATION INFLUENCE IN THE SHORT INTERCAVITY REGIME

When the injection delay time between two mutually coupled semiconductor lasers is much smaller than the relaxation oscillation period, the propagation phase $\varphi_0 = \Omega\tau \mod 2\pi$ becomes a critical parameter in the system. In our case of mutually coupled VCSEL's, we study how this phase affects the dynamics of each polarization mode and what is the influence of the spin-flip rate. In Figure 3, we show the bifurcation diagrams of the optical power associated to the four polarization modes, when the propagation phase has been taken as the bifurcation parameter.

In this first case ($\gamma_s = 50$ ns^{-1}), we observe how changing the propagation phase, chaotic, periodic and steady states can be selected for the dominant polarization ($\hat{y}$-modes) of each VCSEL, by just slightly modifying

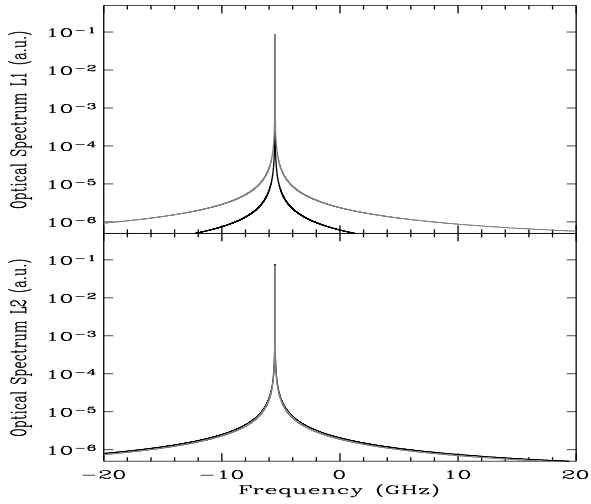

Figure 2. Optical spectra of the polarization modes under frequency locked operation. Black and grey distinguish the $\hat{x}$-modes from the $\hat{y}$-modes.

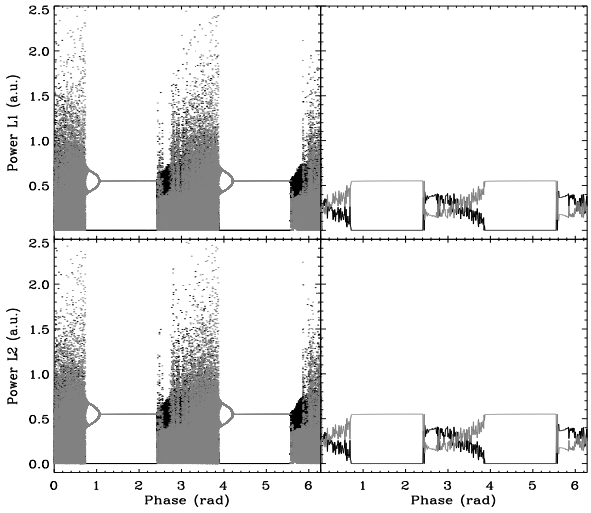

Figure 3. Left panel contains bifurcation diagrams for the optical power of the two polarization modes of both lasers. Right panel shows the mean value of the left panel series when averaged over 50 ns. Black and grey distinguish the $\hat{x}$-modes from the $\hat{y}$-modes. Other parameters are $\mu = 1.5$, $\kappa = 10$ ns^{-1}, $\tau = 0.2$ ns and $\Delta = 0$. A low spin-flip rate is considered here, $\gamma_s = 50$ ns^{-1}.

the distance between lasers. Regarding the less powerful $\hat{x}$-modes, it is clear that only at certain values of the phase they may become active, while for other regions they are strongly suppressed. It is also noticed that the polarization in both lasers behaves identically.

Increasing the spin-flip rate up to $\gamma_s = 400$ ns^{-1}, we found a very different behavior from the analyzed in the previous case, as it can be observed in Figure 4. Now, a constant optical power of each polarization mode is found for almost all the phase values. Only narrow periodic windows are centered around selected values of

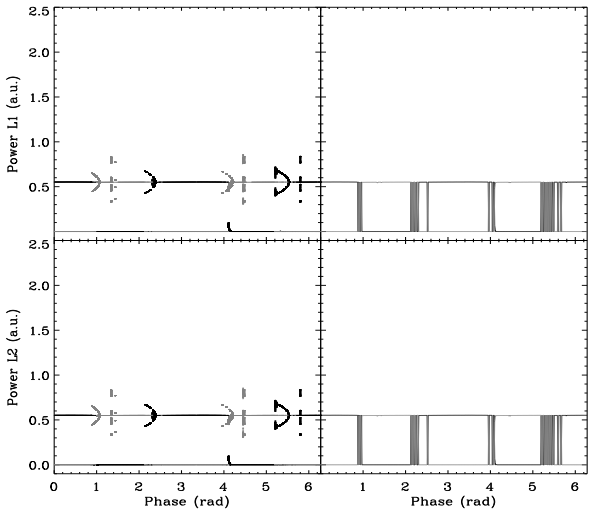

Figure 4. Left panel contain bifurcation diagrams for the optical power of the two polarization modes of both lasers. Right panel shows the mean value of the left panel series when averaged over 50 ns. Black and grey distinguish the $\hat{x}$-modes from the $\hat{y}$-modes. Same parameters than those used in Figure 3, except $\gamma_p = 400$ ns^{-1}.

the propagation phase. However, one of the main differences is related to the fact that a change in the phase may induce a switching between the dominant modes, i.e., depending on the specific phase value, the dominant polarization can be the $\hat{x}$ or the $\hat{y}$-mode. Several of these transitions are illustrated in the Figure 4. We also point out that generically, when a mode becomes dominant the other one hardly carries any optical power.

4. NUMERICAL STUDY OF THE POLARIZATION DYNAMICS IN THE COUPLING-DETUNING PLANE

Under this section, we collect some numerical simulations in order to characterize the behavior of the system in the two-parameter space defined by the coupling and detuning coefficients. The effect of the distance between lasers will be also discussed.

First of all, we focus our attention on the mean optical power extracted by each polarization mode, as function of the coupling and detuning values. Figure 5 shows the optical power averaged over 50 ns for the $\hat{x_1}, \hat{y_1}, \hat{x_2}$ and $\hat{y_2}$, modes, when considering a short injection delay time $\tau = 0.2$ ns and a low spin-flip rate $\gamma_s = 50$ ns^{-1}. Hereafter, the pumping current will be fixed to $\mu = 1.5$. When uncoupled, for the set of parameters chosen, each VCSEL is mainly emitting in its $\hat{y}$ polarization mode. This situation, where the predominant mode is the $\hat{y}$ one, is maintained in a neighborhood of the uncoupled zero-detuning state. However, as seen in the Figure 5, if we allow for a large detuning in the low coupling limit, then it is the $\hat{x}$-mode which becomes dominant in both lasers. As it can be observed, this phenomenom occurs for both signs of the detuning value. It is also noticed a kind of periodic structure when increasing the coupling strength while keeping the detuning at small values. So, repetitively the $\hat{y}$-mode pass through a serie of maxima and minima levels with a complementary behavior of its $\hat{x}$-polarized counterpart. Consequently, under the actual conditions, coexistence or strongly suppressed $\hat{x}$-mode polarization states can be obtained by changing the coupling coefficient.

In the case that the long distance limit between the VCSEL's is considered (see Figure 6), we find the same kind of detuning-induced change of the dominant mode for low coupling rates. However, now we observe a monotonic behavior of polarization optical powers when increasing the coupling, contrarily to what happens in the previous case where a periodic structure was revealed.

In order to illustrate the dynamics at some points of the former Coupling-Detuning plane, where only averaged powers were computed, we show in Figure 7 the temporal series and optical spectra corresponding to several

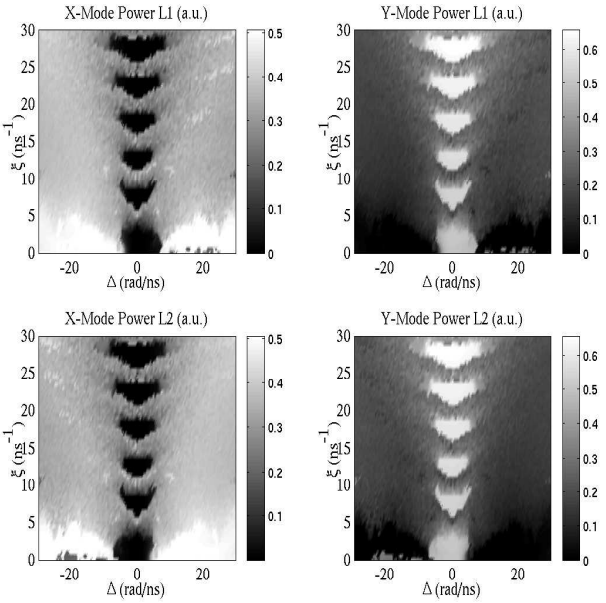

Figure 5. Mean optical polarization-resolved power in the Coupling-Detuning plane. The average has been taken over 100 ns of temporal evolution. Short distance limit ($\tau = 0.2$ ns). Other parameters are: $\mu = 1.5$, $\gamma_s = 50$ ns^{-1} and $\varphi = 0$.

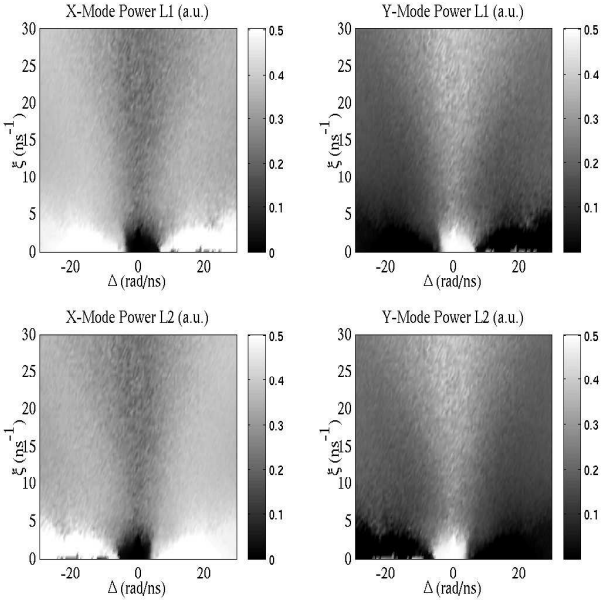

Figure 6. Mean optical polarization-resolved power in the Coupling-Detuning plane. The average has been taken over 100 ns of temporal evolution. Long distance limit ($\tau = 4$ ns). Other parameters are: $\mu = 1.5$, $\gamma_s = 50$ ns^{-1} and $\varphi = 0$.

simulations in the short intercavity regime, where the detuning has been varied. Although a very low coupling was chosen ($\xi = 3$ ns^{-1}), aperiodic oscillations are found even in the absence of detuning for the $\hat{y}$-mode of each laser, while the $\hat{x}$-mode remained completely inactive in both VCSEL's. As the detuning is increased, the coexistence of both modes in each laser exhibiting irregular oscillations leads to a polarization state of the light, that is continously moving over a large portion of the Poincare sphere surface (see Figure 8). Further increasing

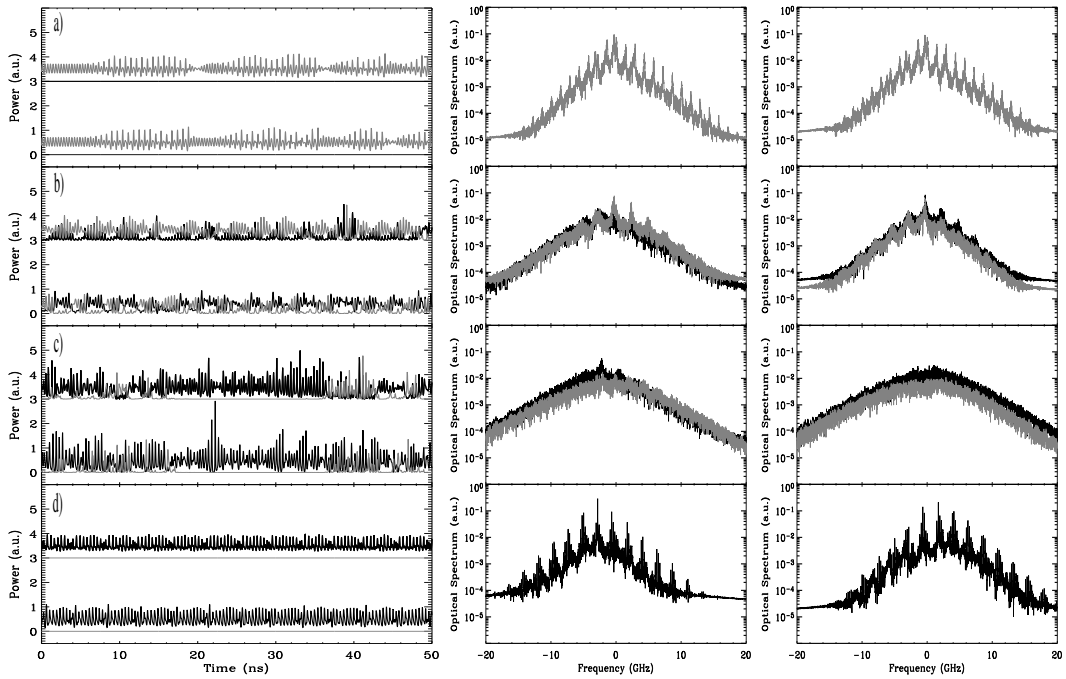

Figure 7. Left panel: temporal series of the $\hat{x}$ and $\hat{y}$-modes for detunings a) $\Delta = 0$, b) 5, c) 10 and d) 15 rad/ns. VCSEL 1 traces have been vertically shifted for clearness reasons. Center panel: Optical spectra for the Laser 1 polarization modes. Right panel: Optical spectra for the Laser 2 polarization modes. The coupling strength have been fixed to $\kappa = 3$ ns^{-1}. The rest of parameters are the same than those used in Figure 5.

the detuning, the $\hat{y}$-mode of each laser is switched-off while the $\hat{x}$-mode evolves in a quasiperiodic state.

5. CONCLUSIONS

In this paper, we have explored the polarization resolved dynamics of two mutually coupled VCSEL's. Focusing on the LFF regime, we have observed how detuning is able to switch the dominant polarization mode of the lower frequency VCSEL. Moreover, frequency locked states were also clearly identified for moderate values of detuning. Similar behavior was found for low and high spin-flip rates. Regarding the role of the propagation phase between the lasers in the dynamics of the system, we adjusted the injection delay time to a very short one and scanned the phase in a typical bifurcation diagram. The results pointed out that for high spin-flip rates, a sudden switch in the dominant polarization mode can be induced by slightly changing the intercavity phase. Finally, we performed extensive numerical simulations varying the coupling rate and the detuning. As future work, we consider the generalization of the present results to a situation in which the principal axis of both lasers are not perfectly aligned, i.e. when a VCSEL is rotated with respect to the other one.

ACKNOWLEDGMENTS

The authors acknowledge financial support from the Ministerio de Ciencia y Tecnología (Spain) and FEDER and BFM2002-04369) and from the EC project IST-2000-29683 OCCULT. C.R.M. is also grateful for the hospitality and support of the Electrical Engineering Department, University of California, Los Angeles. C.R.M is also funded by the Secretaría de Estado de Educación y Universidades, Ministerio de Educación, Cultura y Deporte, Spain.

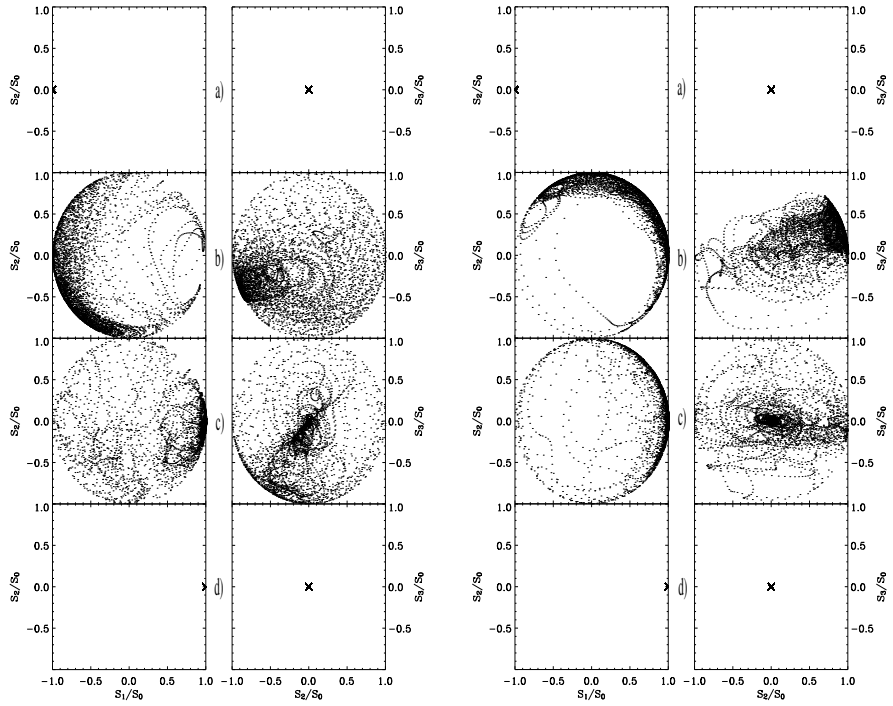

Figure 8. Evolution of the polarization in the Poincare sphere projections corresponding to the temporal traces in Figure 7. Left and right panels collect the results for the laser 1 and 2, respectively.

REFERENCES

1. N. A. Loiko, A. V. Naumenko, and N. B. Abraham, "Complex polarization dynamics in a vcsel with external polarization-selective feedback," *J. Opt. B: Quantum Semiclass. Opt.* **3**, p. 100, 2001.
2. M. Sciamanna, F. Rogister, O. Deparis, P. Megret, and B. M., "Bifurcation to polarization self-modulation in vertical-cavity surface-emitting lasers," *Optics Lett.* **27**, p. 261, 2002.
3. P. Spencer, C. R. Mirasso, P. Colet, and A. Shore, "Modeling of optical synchronization of chaotic external-cavity vcsel's," *IEEE J. of Quantum Electron.* **34**, p. 1673, 1998.
4. N. Fujiwara, Y. Takiguchi, and J. Ohtsubo, "Observation of the synchronization of chaos in mutually injected vertical-cavity surface emitting semiconductor lasers," *Optics Lett.* **28**, p. 1677, 2003.
5. M. San Miguel and J. V. Feng, Q. Moloney, "Light polarization dynamics in surface emitting semiconductor lasers," *Phys. Rev. A* **52**, p. 1728, 1995.
6. H. T., I. Fischer, W. Elssser, J. Mulet, and C. Mirasso, "Chaos synchronization ans spontaneous symmetry-breaking in symmetrically delay-coupled semiconductor lasers," *Phys. Rev. Lett.* **86**, p. 795, 2001.